

Reference

NBS
Publi-
cations



A11104 551605

NBSIR 79-1620

TIME DOMAIN PULSE MEASUREMENTS AND COMPUTED FREQUENCY RESPONSES OF OPTICAL COMMUNICATIONS COMPONENTS

James R. Andrews

Matt Young

Electromagnetic Technology Division
National Engineering Laboratory
National Bureau of Standards
Boulder, Colorado 80303

September 1979

QC
100
.U56
79-1620
1979

NBSIR 79-1620

TIME DOMAIN PULSE MEASUREMENTS AND COMPUTED FREQUENCY RESPONSES OF OPTICAL COMMUNICATIONS COMPONENTS

James R. Andrews
Matt Young

Electromagnetic Technology Division
National Engineering Laboratory
National Bureau of Standards
Boulder, Colorado 80303

September 1979



U.S. DEPARTMENT OF COMMERCE, Juanita M. Kreps, Secretary
Luther H. Hodges, Jr., Under Secretary
Jordan J. Baruch, Assistant Secretary for Science and Technology
NATIONAL BUREAU OF STANDARDS, Ernest Ambler, Director

CONTENTS

Abstract.....	1
Introduction.....	1
Background.....	1
Lasers.....	2
Photodiodes.....	3
Automatic Pulse Measurement System.....	4
Experiment Confirgurations.....	4
Test Fibers.....	6
Fiber Measurement Results.....	7
Impulse and Frequency Response of an Avalanche Photodiode.....	9
Acknowledgments.....	9
Figures.....	10
APPENDIX A.....	26
APPENDIX B.....	29
REFERENCES.....	31

TIME DOMAIN PULSE MEASUREMENTS AND COMPUTED FREQUENCY RESPONSES
OF OPTICAL COMMUNICATIONS COMPONENTS

James R. Andrews and Matt Young

The purpose of this report is to demonstrate the application of the NBS Automatic Pulse Measurement System (APMS) to measuring the pulse responses of optical communications components and to computing their impulse and frequency responses. For example we describe measurements of the properties of two glass fibers and an avalanche photodiode using both a pulsed GaAs laser diode ($\lambda = 0.9 \mu\text{m}$) and a mode locked, Nd:YAG laser ($\lambda = 1.06 \mu\text{m}$). All measurements were performed in the time domain; frequency domain data were obtained from the time domain data by using the Fast Fourier Transform (FFT). The impulse response was obtained by deconvolution.

Key Words: Avalanche photodiode; FFT; fiber optics; frequency response; impulse response; laser; photodiode.

Introduction

The purpose of this report is to demonstrate some techniques for pulse measurements on optical communications components and the application of the NBS Automatic Pulse Measurement System (APMS) to such measurements. The components tested included step index and graded index fibers and an avalanche photodiode. Using short pulse laser inputs, we used the APMS to measure the transient responses of the various components in the time domain. The APMS is a dc-18 GHz sampling oscilloscope interfaced with and controlled by a dedicated mini-computer. From the time domain data we derived frequency domain information on the APMS minicomputer using the Fast Fourier Transform (FFT). Both magnitude and phase data were computed to describe the transfer function, the insertion loss $S_{21}(f)$ and the frequency response. We derived the impulse response by a deconvolution technique. The lasers used included a pulsed GaAs laser diode ($\lambda = 0.9 \mu\text{m}$) and a mode locked, Nd:YAG laser ($\lambda = 1.06 \mu\text{m}$). The laser pulse durations were approximately 130 ps and 80 ps respectively.

Background

When the field of fiber optics for telecommunications was still in its infancy, the importance of light pulse distortion in fibers was recognized by systems designers as a major problem. Early NBS work in this field was done in cooperation with the Centre National d'Etudes des Telecommunications (CNET) in Lannion, France. The NBS-CNET research involved measuring the pulse distortion in the high loss optical fibers available at that time [1]. High temporal resolution (~ 100 ps) measurements were made using GaAs and argon lasers. The measurements and results were all in the time domain. However, it was foreseen at the time [1] that much more information could be obtained from the time domain measurements when it would be possible to use computer processing and Fast Fourier Transforms (FFT). Since that time, the use of time domain, short pulse measurements and

computed FFTs has become the most commonly used technique to determine the pulse distortion and bandwidth of optical fibers [2-6]. They are part of a Military Standard first drafted in 1976 [7].

The early CNET-NBS work developed an avalanche transistor circuit to pulse a GaAs laser diode and demonstrated that a short (~ 100 ps) light pulse could be obtained from such a laser [1,8]. In 1974 an improved circuit was reported [9]. This circuit and variations have been widely used since then by many laboratories and companies interested in short pulse testing of optical fibers and is reproduced here as Appendix A. This report includes a newly modified version of the 1974 circuit.

Many of the basic techniques of time domain testing of optical fibers are now well known, although many problems remain. This report is intended in part to demonstrate our capability in this area. In addition we document some unusual multimode waveforms encountered in a graded index fiber when tested with the NBS, high temporal resolution (~ 100 ps), $1.06 \mu\text{m}$ test apparatus.

Lasers

We used two lasers; the first was a pulsed GaAs laser diode. This laser pulse generator is described in detail in Appendix B. It is a modification of an earlier version [9]. Laser diode A¹ emits at a wavelength of $0.9 \mu\text{m}$. It has a peak forward current rating of 10 A and a typical threshold of 4 A. With certain selected diodes, optical pulses as narrow as 110 ps have been observed [9].

To obtain close coupling to a fiber, we removed the protective, glass face plate of the laser. This allowed the fiber to be placed extremely close to the output face of the laser. The fiber was not allowed to touch the laser because this drastically detuned the cavity and altered the laser's output characteristics.

The $1.06 \mu\text{m}$ laser was a continuously mode locked, commercial YAG laser that we have stabilized with quartz rods. The length of the cavity is about 2 m and the corresponding pulse repetition frequency 100 MHz (or, equivalently, the period of the pulses is 10 ns). The average output power, measured at the output mirror, is 1 W.

We have measured the duration of the pulses using an autocorrelation technique [10]. The apparatus consists of a Michelson interferometer [11] that is modified by replacing its plane mirrors with right angle (Porro) prisms. The modification prevents the beam reflected by the interferometer from propagating back into the laser and thereby interfering with the mode locking process. The beam that emerges from the interferometer is focused with careful alignment into a second harmonic generating crystal; the 530 nm radiation is

¹ Due to NBS policy, manufacturers' names and model numbers are omitted to avoid any endorsement.

detected with a silicon photocell and a colored glass filter suitable for blocking the 1.06 μm radiation. We use an xy recorder connected to the output of the photocell and to the moveable arm of the interferometer to record the autocorrelation function of the pulses.

The duration of the autocorrelation function is 0.11 ns. The duration of the pulses themselves cannot be determined precisely from an autocorrelation measurement [10]. If the pulses are roughly gaussian in shape, then the pulse duration is 0.707 times the duration of the autocorrelation function; for our pulses, this yields durations of about 0.08 ns. The peak pulse power is therefore approximately 125 W.

Photodiodes

We tested and used several photodiodes, including PIN and avalanche, Si and Ge, which were either commercial or research devices.

To determine the output of the laser diode we used an experimental, epitaxial Si photodiode built by the Centre National d'Etudes des Télécommunications (CNET). The waveform obtained is shown in figure 1. The 50% duration (FWHM) of the first pulse is 0.14 ns. The minor bump (100 ps after the first pulse) is attributed to an internal reflection within the photodiode mount, whereas the second major pulse (300 ps later) is a feature of the laser. When driven with a long pulse, lasers A produce a train of relaxation oscillations with spacing of the order of 1/3 ns.

Previous tests of the CNET photodiode at 600 nm with a ~ 10 ps, mode locked dye laser resulted in waveforms whose duration was about 70 ps. Although photodiode impulse responses will vary with wavelength, the 70 ps value can be used for a rough estimate of the pulse duration t_ℓ of laser A. We assumed that the measured waveform was the convolution of the laser pulse with the impulse responses of the photodiode and the sampling oscilloscope. The squares of the durations of each add roughly to yield the square of the duration of the observed waveform. Thus,

$$t_\ell = (t_{\text{meas}}^2 - t_{\text{pd}}^2 - t_{\text{so}}^2)^{1/2}, \quad (1)$$

where t_{meas} is the observed 0.14 ns impulse duration, t_{pd} is the assumed 55 ps impulse duration of the photodiode, and t_{so} is the 19 ps impulse duration of sampling oscilloscope C. With these values in eq. (1) we estimate that laser A's pulse duration is approximately 0.13 ns.

For fiber measurements at 0.9 μm , we used a fast, commercial, avalanche photodiode (APD, designated D) because of its greater responsivity than the CNET Si photodiode. The response of this diode to laser A consists of a fast pulse (0.35 ns, 50% duration) followed by a slow tail, as shown in figure 2.

A slower, commercial avalanche photodiode (E) was also tested to determine its impulse and frequency responses. This measurement is described in a later section.

We used two different photodiodes at 1.06 μm . The faster was a CNET Ge photodiode [1,12]. Figure 3 shows its output when irradiated by the YAG laser. The duration of the

main impulse is 0.12 ns, the YAG laser pulse having been degraded somewhat by transmission through the 10 m fiber pigtail used to bring the laser pulse from the laser room into the APMS room. We estimate the impulse response duration (FWHM) of the photodiode to be of the order of 0.09 ns. [1].

Measurements were also made at 1.06 μm with a commercial, Si PIN photodiode (F) whose pulse response is shown in figure 4. The duration is 0.37 ns. It is characterized by a fast leading edge and a slower trailing edge. In this case the diode's response is considerably slower than the YAG laser; therefore, figure 4 is a close approximation to the diode's impulse response.

Automatic Pulse Measurement System

The time domain measurements were made with the NBS Automatic Pulse Measurement System (APMS) [4,5,13]. The APMS is basically a wideband (dc - 18 GHz), 20 ps transition time, sampling oscilloscope interfaced with and controlled by a dedicated minicomputer (figure 5). The oscilloscope was modified by NBS to permit computer control; an analog signal averager was also added to the oscilloscope to reduce its noise level from 5 mV to 500 μV . In addition, the minicomputer performs digital signal averaging; therefore, it is possible to measure low level signals with high signal-to-noise ratio. Once a signal is acquired and stored in the computer's memory or auxiliary floppy disc, it can be processed at any later time. For example, when we are interested in frequency domain properties, such as the spectrum amplitude of a signal or the attenuation of a component, then the minicomputer uses the Fast Fourier Transform (FFT) to transform the data from the time domain to the frequency domain. The minicomputer can also perform deconvolution to determine an unknown network's impulse or step response.

Experiment Configurations

The experimental setups for measurements on glass fibers are shown in figures 6 and 7 for each of the two wavelengths used.

At 0.9 μm , we used laser diode A as the optical pulse generator. The light output from the laser was collected by the 80 μm , 0.14 NA glass fiber held 0.1 mm from the laser's emitting surface by a micropositioner. The output from the fiber was focused onto avalanche photodiode D. The photocurrent pulse was sent to sampler C through a 60 ns delay line I. At the input to the delay line a trigger signal was picked off by a 6 dB power divider tee for triggering the sampling oscilloscope time base. The delay line reduced the effective oscilloscope bandwidth to 3 GHz, which is adequate for these measurements.

An alternate technique would take the signal from the APD directly to the sampler and trigger the oscilloscope from the pulse generator. However, with kilometer long fibers, time delays of the order of microseconds are encountered. In these situations a long electronic time delay network must be used between the driving pulse generator and the trigger input to the oscilloscope. Quite stringent requirements are imposed on this delay network, because it must provide microsecond delays with less than 20 ps of jitter. The delay line method of figure 6 is an easy way around this problem.

We used an insertion technique to measure the response of a long fiber. First the response waveform $v_1(t)$ of the measurement system was acquired by the APMS, with a short, 30 cm piece of fiber between the laser diode and the APD. This waveform includes the convolved effects of laser, APD, fiber, delay line and sampler. To avoid saturation and non-linearity in the APD, a density 1.0 filter was placed between the fiber output and the lens when the short fiber was measured. Then, using the micropositioners, we replaced the 30 cm fiber with the long fiber to be tested. The new waveform $v_2(t)$ was also measured by the APMS.

The magnitude and phase of the insertion loss S_{21} ,

$$S_{21}(f) = \frac{\text{FFT } v_2(t)}{\text{FFT } v_1(t)} \quad (2)$$

of the long fiber were calculated by the minicomputer. From $v_1(t)$ and $v_2(t)$ the minicomputer also computed the impulse response of the fiber by deconvolution.

Figure 7 shows the experimental setup used for the 1.06 μm laser measurements. The YAG laser produced a train of mode locked pulses with the repetition rate of 100 MHz (as opposed to the 50 kHz of the laser diode). The output of the laser was focused onto the core of a 10 m step index fiber with a 5X microscope objective. The numerical aperture of the microscope objective was specified by the manufacturer as 0.10; therefore, the spot diameter at the focus of the objective was of the order of 10 μm [11] or significantly less than the fiber's core diameter.

The laser and the 10 m fiber pigtail became the source for our measurements on the longer fiber cables. We used a 10X, 0.25 NA microscope objective at approximately unit magnification to couple the radiation from the pigtail to the fiber under test. (Whereas this objective was designed for use with a tube length [11] of 160 mm, we used it for our application because it was readily available in a solid mount. A simple calculation shows that it should have been easily able to resolve the exit face of the 80 μm diameter pigtail.) Assuming that the exit face of the fiber pigtail was filled but that mode coupling was insignificant in a 10 m fiber, we conclude that the entrance face of the test fiber was irradiated with a bundle that had a launch numerical aperture of 0.10 (that of the 5X objective). The spot diameter on the entrance face of the test fiber was about 80 μm , equal to the diameter of the exit face of the pigtail.

At the output end of the test fiber, we focused the radiation onto the photodiode with a single element, condensing lens whose focal length was about 17 mm. We used filters to control the total power that fell onto the photodiode.

To measure the pulse response of the laser and the pigtail, we omitted the test fiber and the microscope objective; that is, we used the condensing lens to focus the output of the pigtail directly onto the photodiode.

The output of the CNET, Ge photodiode was sent directly to the input of sampler C. A 6 dB power divider split the output of the sampler into two paths. One signal passed through a broadband amplifier and triggered the oscilloscope; 60 ns later the oscilloscope's sweep started, so the sixth pulse after the trigger pulse was displayed on the screen. The second output from the power divider went to a spectrum analyzer. The spectrum analyzer was, among other things, useful as an alignment tool to help find the signal when it was too small to be observed on the oscilloscope.

Test Fibers

Two fibers were tested in these experiments. One was a 100 m, step index fiber; the other was a 580 m, graded index fiber. Additional specifications are listed in Table I.

Table I

Test Fiber Specifications

<u>Parameter</u>	<u>Fiber G</u>	<u>Fiber H</u>
Type	Step-Index	Graded-Index
Length	100 m	580 m
Core Diameter	80 μm	75 μm
Cladding Diameter	135 μm	125 μm
Cladding Material	SiO ₂	Not specified
Jacketing Material	None	Plastic
Core Index of Refraction	1.5	Not specified
Numerical Aperture	0.14	0.16
Attenuation	< 30 dB/km @ 0.82 μm	< 10 dB/km wavelength unspecified
Pulse Spreading	5-10 ns/km	Not specified

Fiber Measurement Results

We report here the results of experiments on two fibers: (1) 100 m, step index fiber at 0.9 μm and (2) 580 m, graded index fiber at 1.06 μm .

The response of the 100 m, step index fiber to a laser diode pulse is shown in figure 8. Compare this figure with the reference pulse obtained with the short 30 cm fiber, figure 9 (see figure 2 for an expanded time scale). The pulse has been broadened, at the 50% level, by about 1.7 ns.

The insertion loss is computed from these two waveforms using equation (2). The attenuation in dB versus frequency is plotted in figure 10. The APMS computes frequency data to much higher frequencies than shown. We have plotted only those data that we feel are valid. The low frequency attenuation is 1.6 dB/100 m which compares favorably with the manufacturer's specification of < 30 dB/km. The -3 dB effective electrical bandwidth of the fiber is 140 MHz.

In addition to determining the transfer function, one can also use the results of these measurements to calculate the impulse response $h(t)$ of the fiber. Numerical deconvolution of noisy data is a tricky process and must be done with great care to avoid obtaining erroneous results [14]. Using NBS developed deconvolution programs, the APMS computed the impulse response of the 100 m fiber, figure 11. The impulse response can then be integrated over the observation period to give the step response, figure 12. The impulse response has a fast leading edge and a slow tail with a 50% duration of 0.71 ns. The step response has a 2.21 ns transition duration (10%-90%) with the relative 100% level being defined as the last observed amplitude value in the time period. The true 100% level will occur much later in time; note the non-zero slope of the step response near the end of the time period.

We did not cut these fibers to determine their bandwidth versus length characteristics. Many other workers [15, 16] have observed that fibers often exhibit pulse dispersion that is proportional to the length for short lengths (less than the equilibrium coupling length) and that for greater lengths distortion is proportional to the square root of the length.

Using the YAG laser and the CNET Ge photodiode, we also tested a longer (580 m), graded index fiber at 1.06 μm . For this length of fiber and test conditions, the observed output waveforms were slow compared to the input waveform and thus closely approximate the fiber's impulse response. We noted some unusual effects with this fiber. As we scanned the input laser beam across the core, we observed radically changing pulse responses as a function of position. The common feature of these responses was a broad base with a duration of about 1 ns; superimposed on this base were several sharp spikes. The relative amplitudes and positions of the spikes varied rapidly with the position of the beam. At times we saw as many as seven distinct spikes.

Other observers have seen somewhat similar impulse responses, although the spiking behavior was less pronounced owing to longer excitation pulses, and they did not report variations of the impulse response with the manner of excitation [17, 18]. The authors of both references [17] and [18] were able to account for their observations by careful numerical calculation of the impulse response; the calculations were based on accurate measurements of the refractive index profiles. We know of no simple argument that explains the existence of spiking, except for a brief comment in reference [18] that relates their observations with departures of the index profile from a precise alpha profile (irrespective of the value of alpha).

We recorded several pulse response waveforms using various alignment criteria that might be used in the field. All the waveforms are plotted on a scale of 1 ns/div; figure 13 is the reference waveform plotted on the same scale. (See figure 3 for an expanded waveform at 200 ps/cm). The various alignment criteria were:

- (1) Maximum pulse amplitude, figure 14.
- (2) Maximum dc photodiode current, figure 15.
- (3) Minimum amount of superimposed spiking, figure 16.
- (4) Strongest harmonic at 1 GHz, as observed on the spectrum analyzer, figure 17.
- (5) Strongest harmonic at 1.6 GHz (highest frequency observable on the test spectrum analyzer), figure 18.
- (6) "Optimum" overall waveform based upon maximizing the amplitude while minimizing the superimposed fine structure, figure 19.

Figures 20 and 21 show the attenuation and phase of the graded index fiber using the "optimum" waveform, figure 19. The -3 dB frequency is 633 MHz. The phase plot shows a general upward trend that is attributed to a linear phase shift term. Depending upon the oscilloscope triggering adjustment, the relative position of the response waveform in figure 19 will be moved around in the 10 ns observation period relative to the reference waveform, figure 13. The only effect on the results is a change in the linear phase shift term. The attenuation remains completely unchanged. The important phase characteristic in terms of causing waveform distortion is the deviation from the linear phase shift. Further phase data processing can be done by the minicomputer if desired.

Frequency responses were computed for all the waveforms. The attenuation results are summarized in figure 22. All possess a common frequency roll-off characteristic for attenuations less than 10 dB. The total variation in -3 dB bandwidths is less than 7%; major variations occur only in the high frequency characteristics.

These results could have been estimated from a simple inspection of the time domain waveforms. The waveform of figure 16 has essentially no spikes and may be considered as a simple 1 ns pulse. The other waveforms have spikes superimposed on the 1 ns pulse, which carries most of the low frequency information. From Fourier analysis we know that a large number of high frequency components are required to generate a fast transient or "spike". Thus the waveform with the maximum pulse amplitude, figure 14, likewise has the strongest high frequency harmonics (-12 dB at 2.9 GHz) whereas the simple 1 ns pulse waveform has the lowest high frequency harmonics (< -27 dB at 1.3 GHz).

Impulse and Frequency Response of an Avalanche Photodiode

A moderately fast avalanche photodiode (E) was also tested in this series of experiments to determine its impulse and frequency responses. In the measurement setup shown in figure 6, the 30 cm fiber coupled the light from the laser diode to the APD. The reference waveform $v_1(t)$, figure 23, was obtained with APD D and had a duration of 0.33 ns. That diode was then replaced by APD E and the response waveform $v_2(t)$ was measured, figure 24. From these data we see that $v_2(t)$ has a duration of 2.1 ns and closely approximates the impulse duration of E. The curve of attenuation versus frequency was computed by the APMS minicomputer, figure 25. The -3 dB frequency is 240 MHz.

Acknowledgments

We wish to acknowledge the support of the Centre National D'Etudes des Télécommunications, Lannion and Issy-les-Moulineaux, France, who furnished the fast Si epitaxial and Ge photo-diodes as part of a long term cooperative exchange program between NBS and CNET. We also wish to express our thanks to Douglas Franzen, Gordon Day and Bruce Danielson of NBS, who lent us the graded-index fiber. Finally, we greatly appreciate the continued encouragement of our group leader N. S. Nahman.

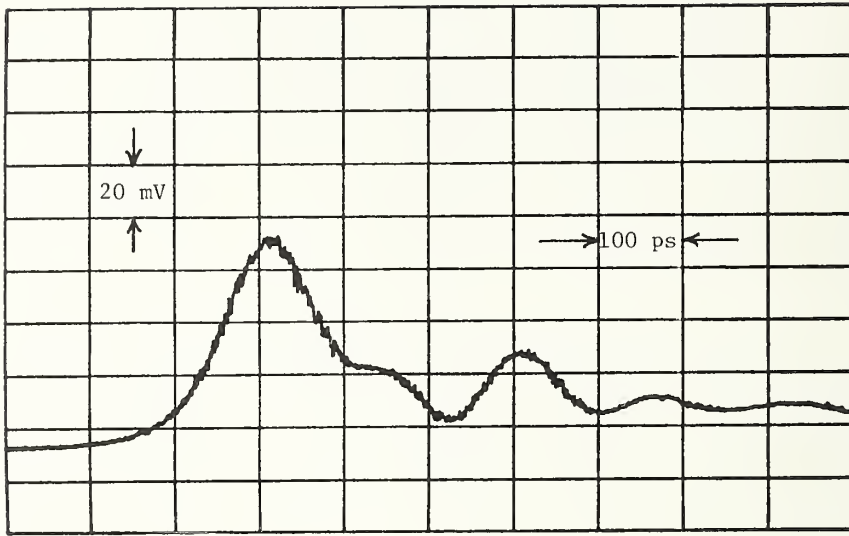


Figure 1. Pulse emitted by laser diode A as observed by the CNET Si photodiode.

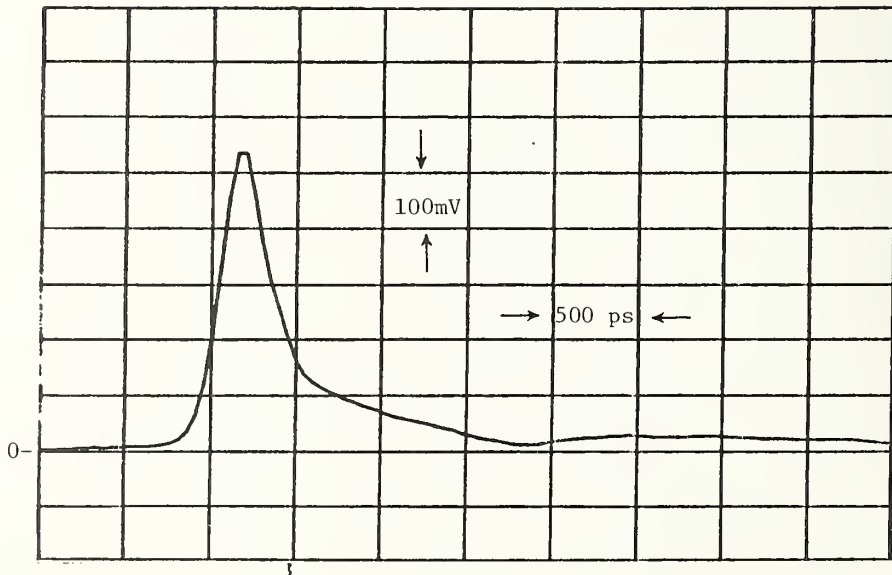


Figure 2. Pulse emitted by laser diode A as observed by the avalanche photodiode D.

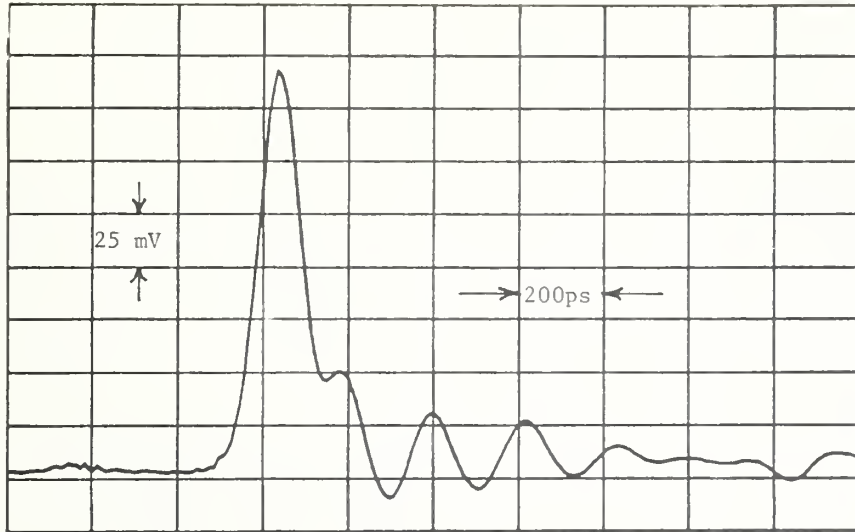


Figure 3. YAG laser output as observed by a CNET Ge photodiode.

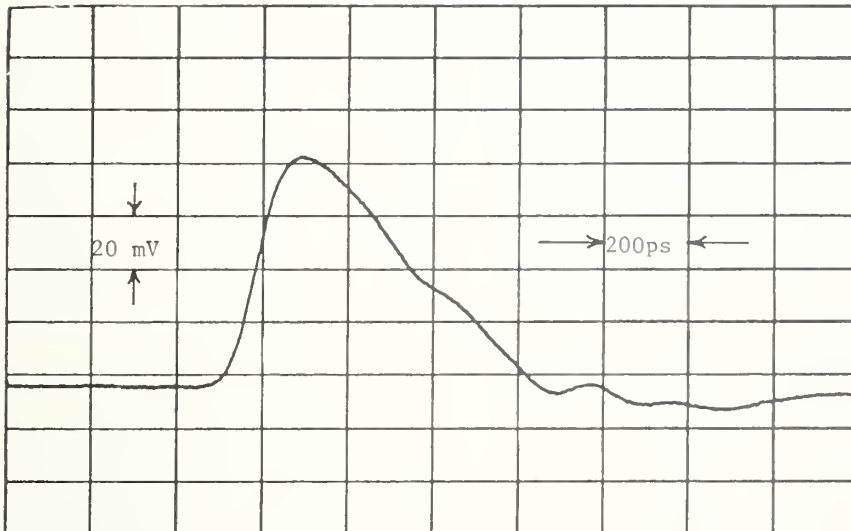


Figure 4. YAG laser output as observed by PIN photodiode F.



Figure 5. The NBS Automatic Pulse Measurement System.

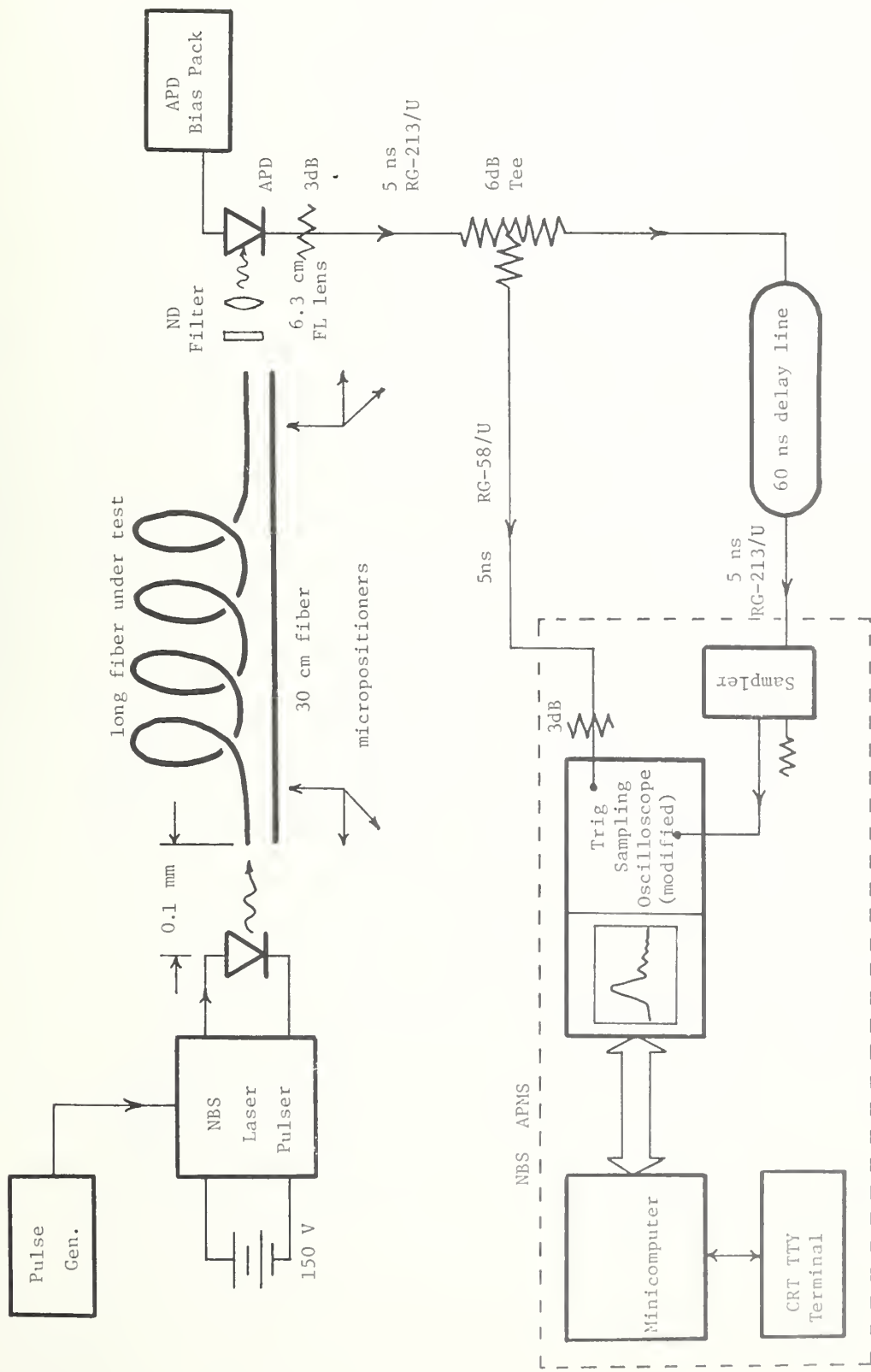


Figure 6. S_{21} test set-up for $0.9 \mu\text{m}$ fiber measurements.

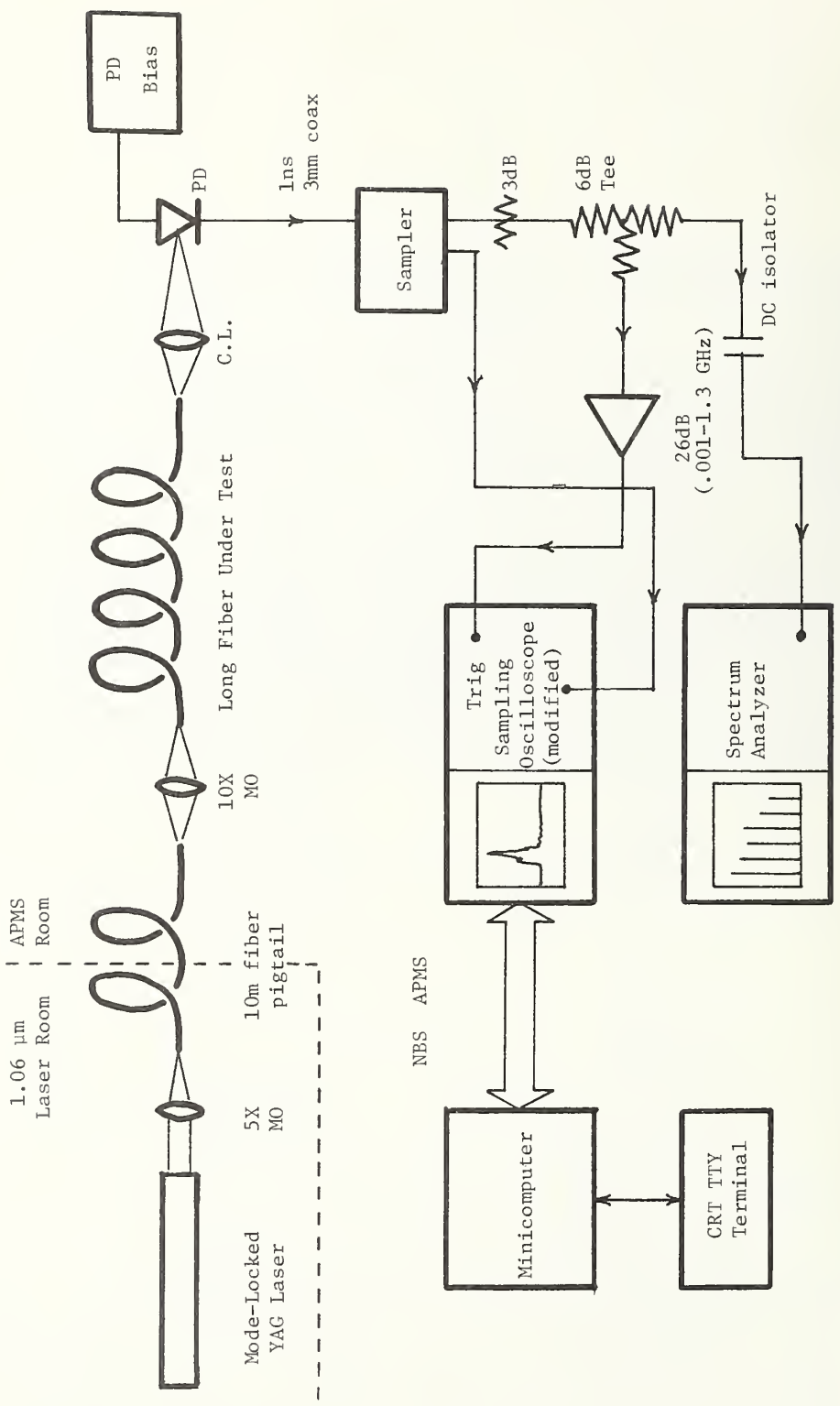


Figure 7. Test set-up 1.06 μm fiber measurements using a Nd:YAG laser.

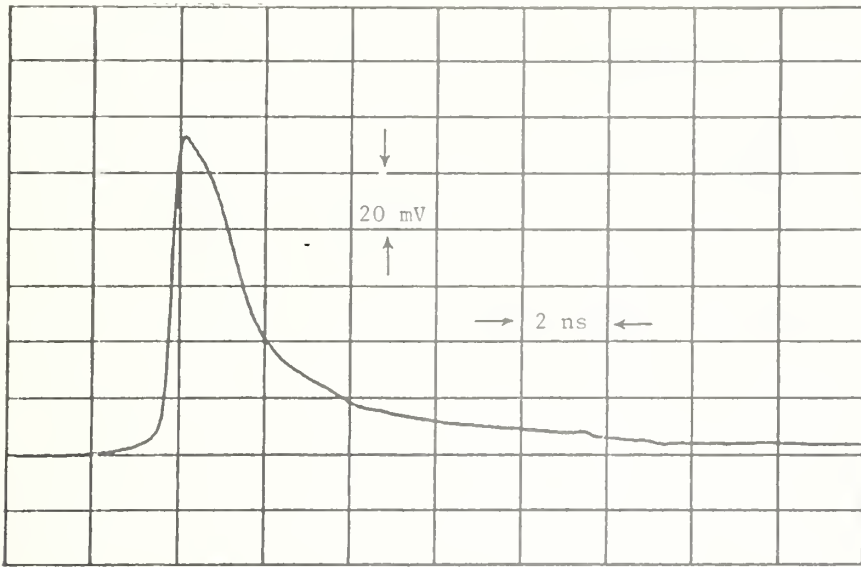


Figure 8. Response of the 100 m step index fiber to the laser diode pulse.

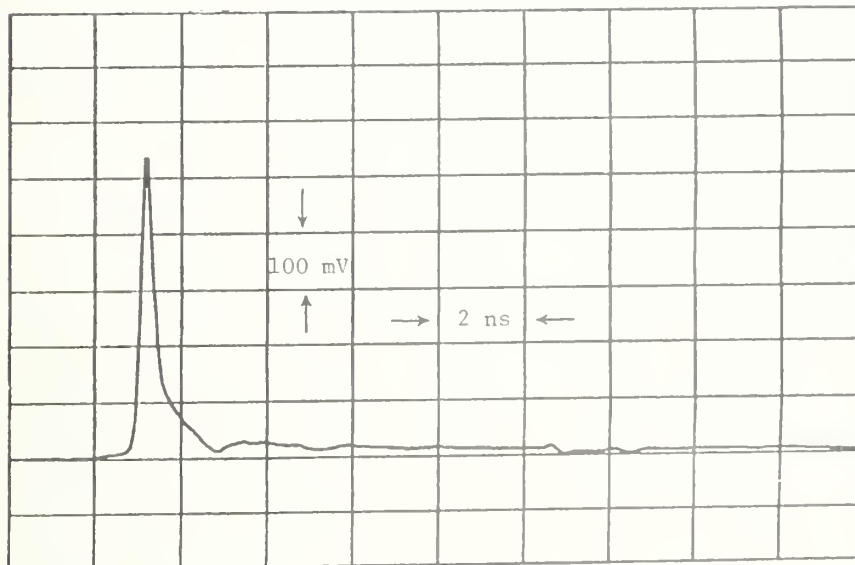


Figure 9. Input reference pulse at 0.9 μm.

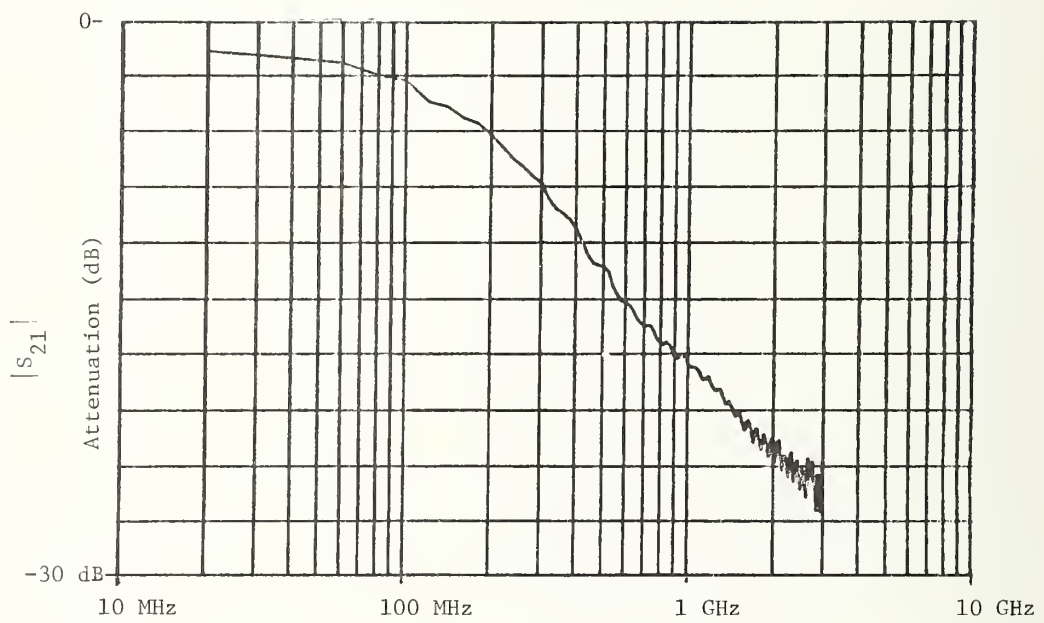


Figure 10. The attenuation versus frequency for the 100 m step index fiber.

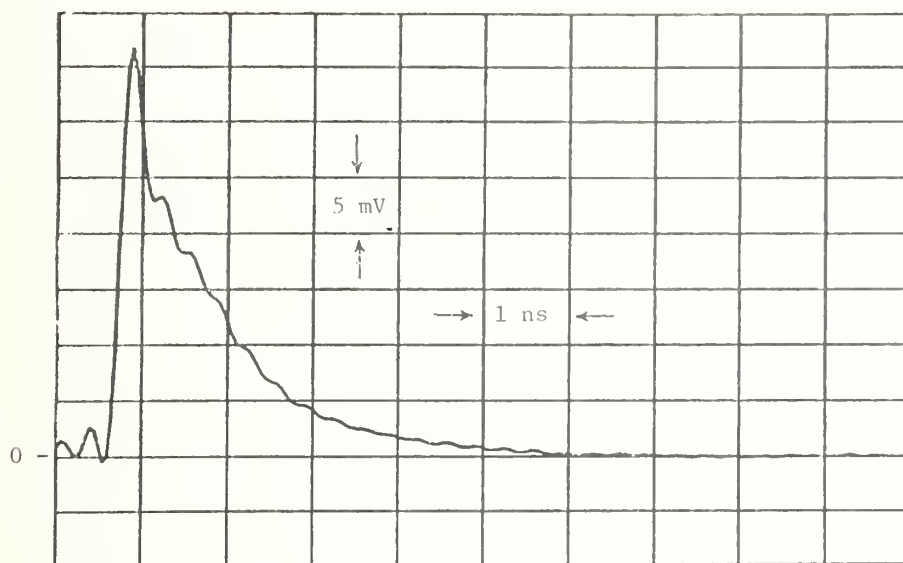


Figure 11. Deconvolved impulse response of the 100 m step index fiber.

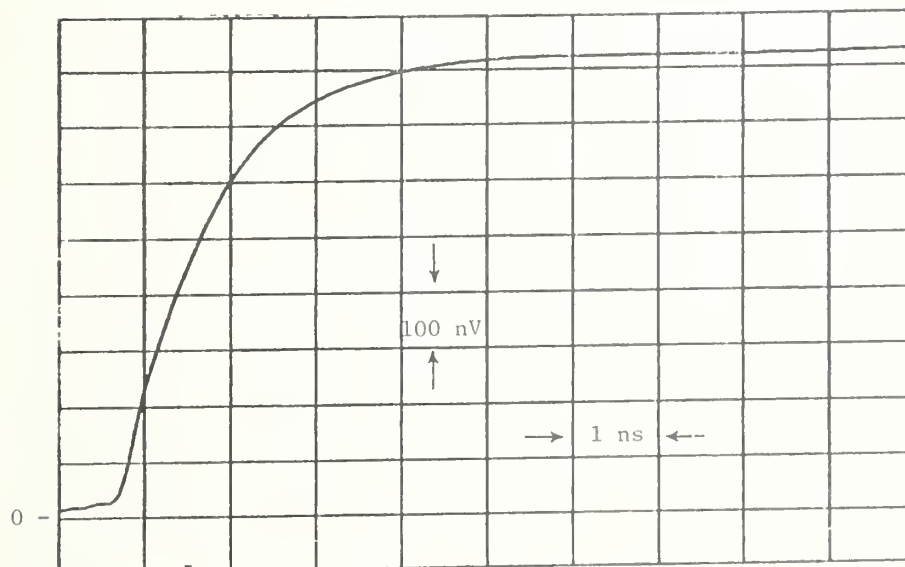


Figure 12. Step response of the 100 m step index fiber.

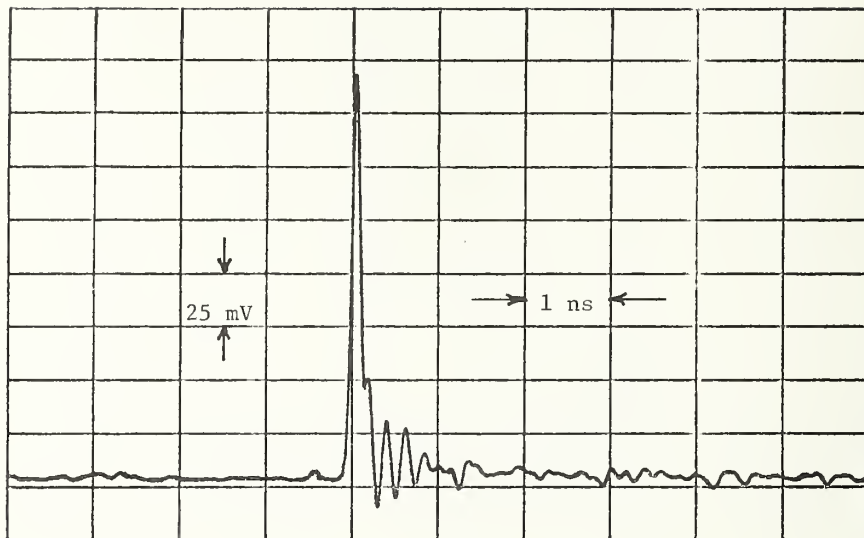


Figure 13. Reference waveform. YAG laser laser pulse into the CNET Ge photodiode.

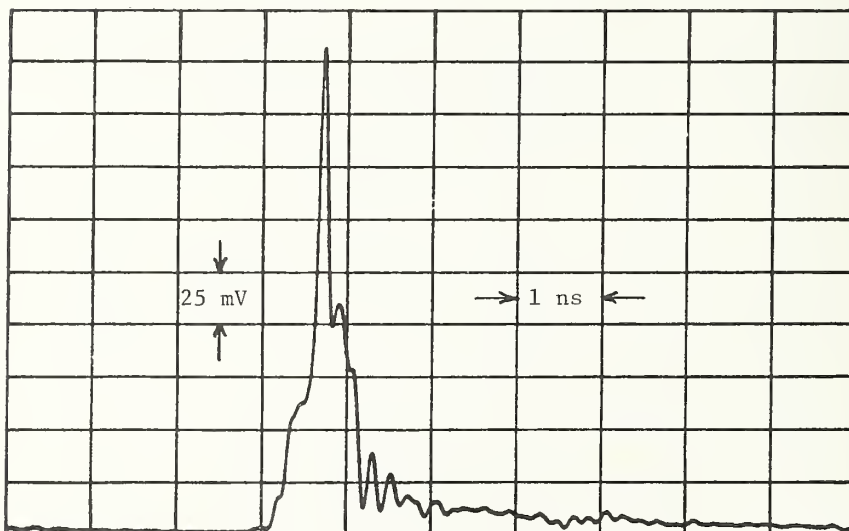


Figure 14. Pulse response of the 580 m graded index fiber. Input launching conditions adjusted for maximum impulse amplitude.

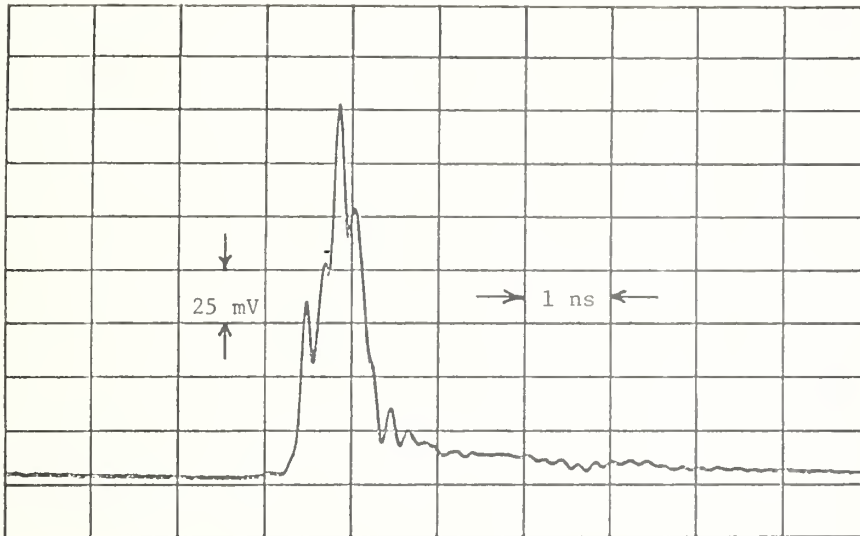


Figure 15. Pulse response of the 580 m graded index fiber. Input launching conditions adjusted for maximum DC photodiode current.

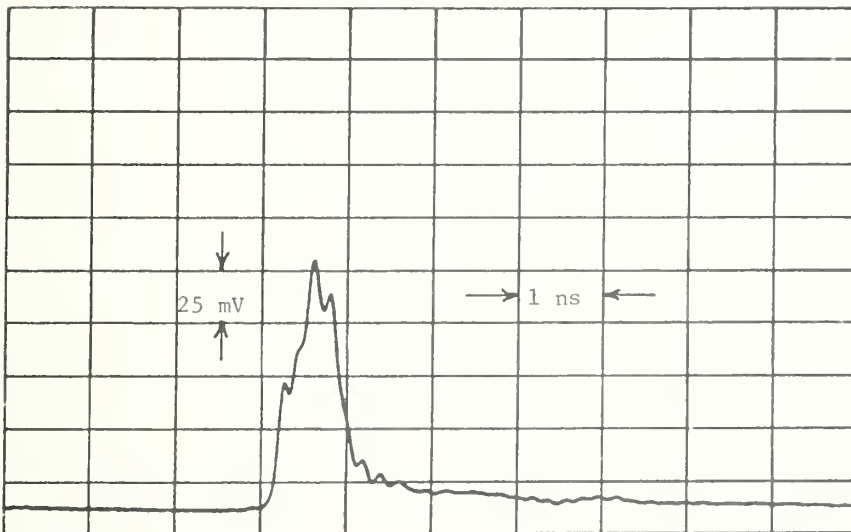


Figure 16. Pulse response of the 580 m graded index fiber. Input launching conditions adjusted for a "square" pulse response with the minimum amount of superimposed "spiking".

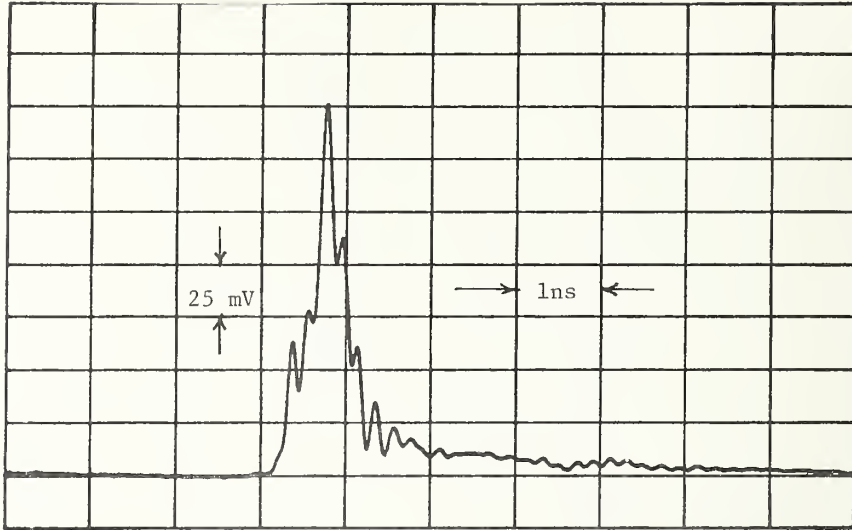


Figure 17. Pulse response of the 580 m graded index fiber. Input launching conditions adjusted for maximum 1 GHz harmonic.

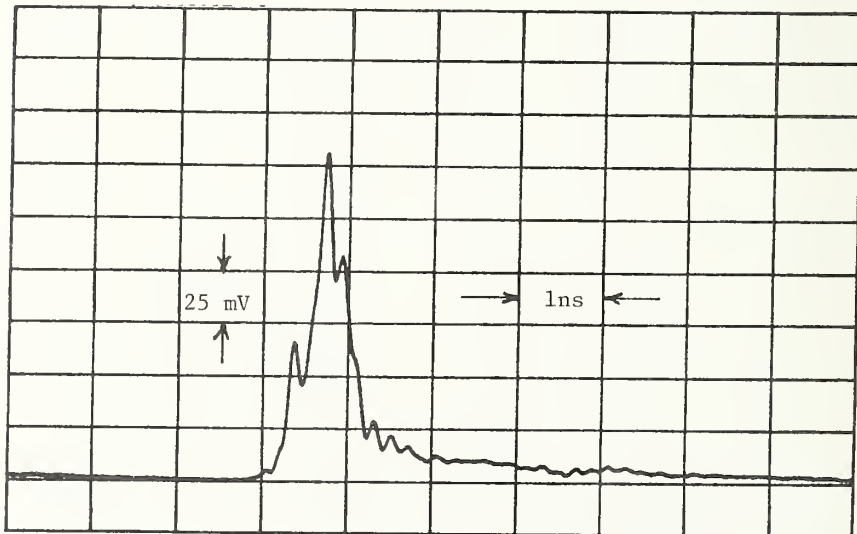


Figure 18. Pulse response of the 580 m graded index fiber. Input launching conditions adjusted for maximum 1.6 GHz harmonic.

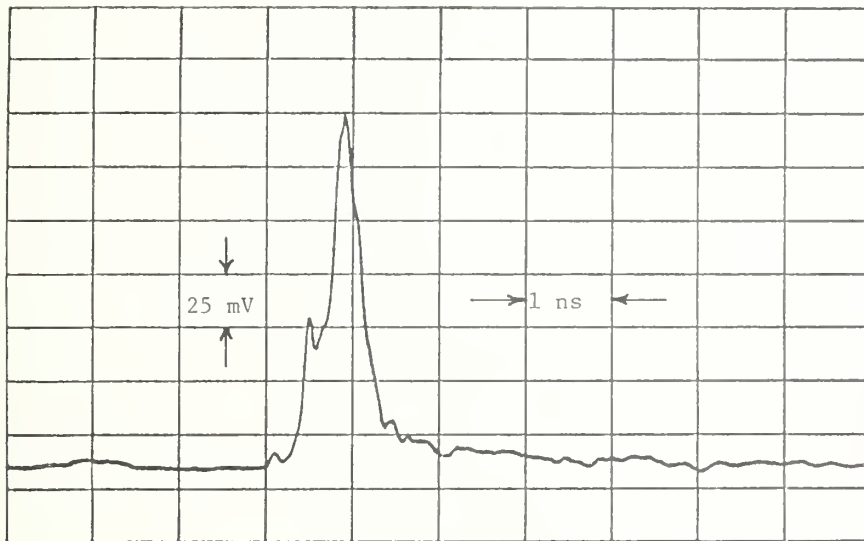


Figure 19. Pulse response of the 580 m graded index fiber. Input launching conditions adjusted for "optimum" output pulse based upon maximizing the amplitude while minimizing the superimposed fine structure.

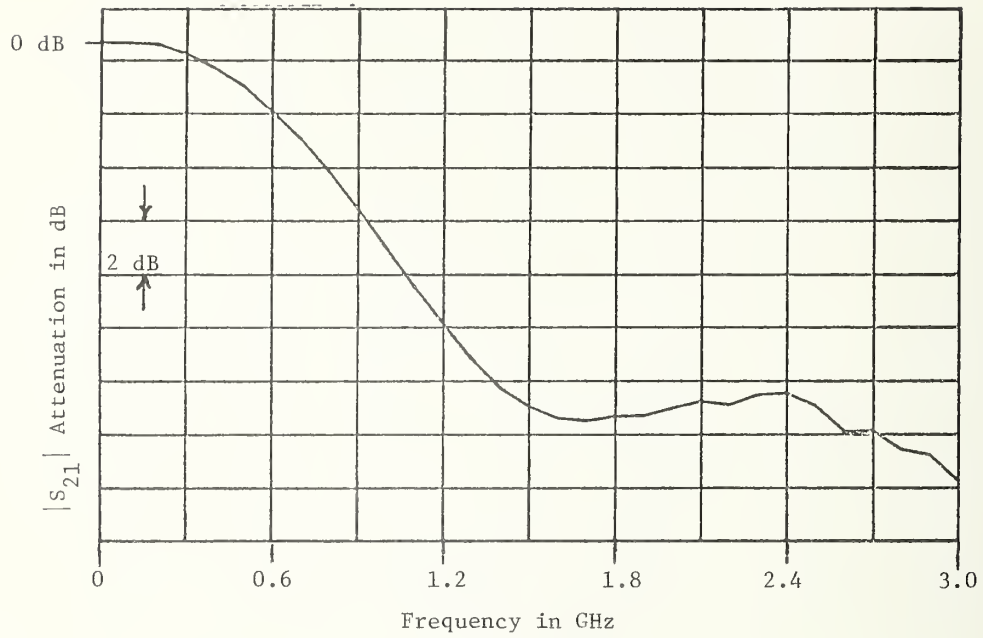


Figure 20. Relative attenuation, $|S_{21}|$, versus frequency.

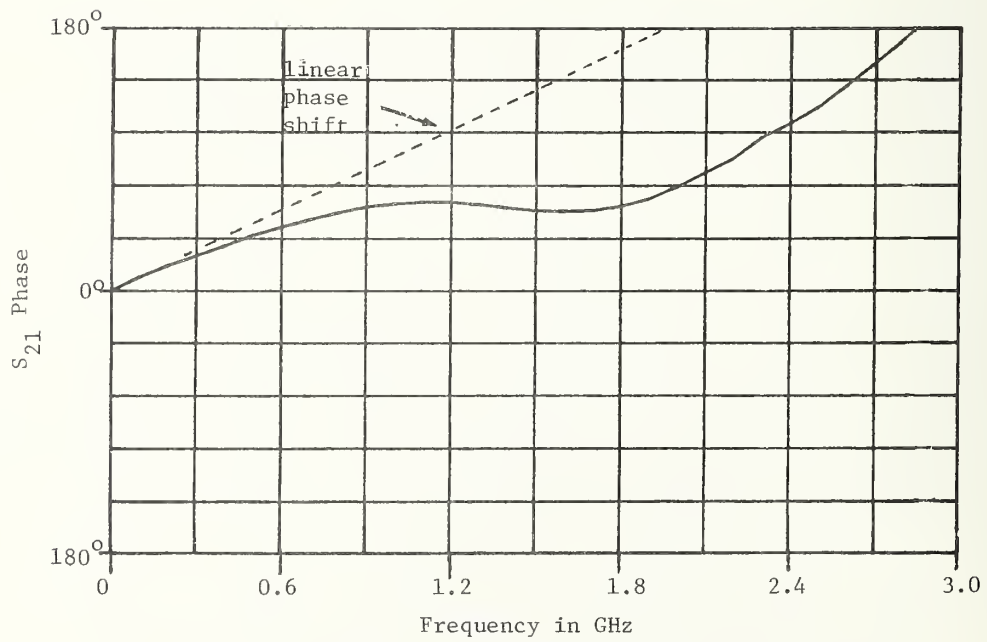


Figure 21. S_{21} phase response of 580 m graded index fiber.

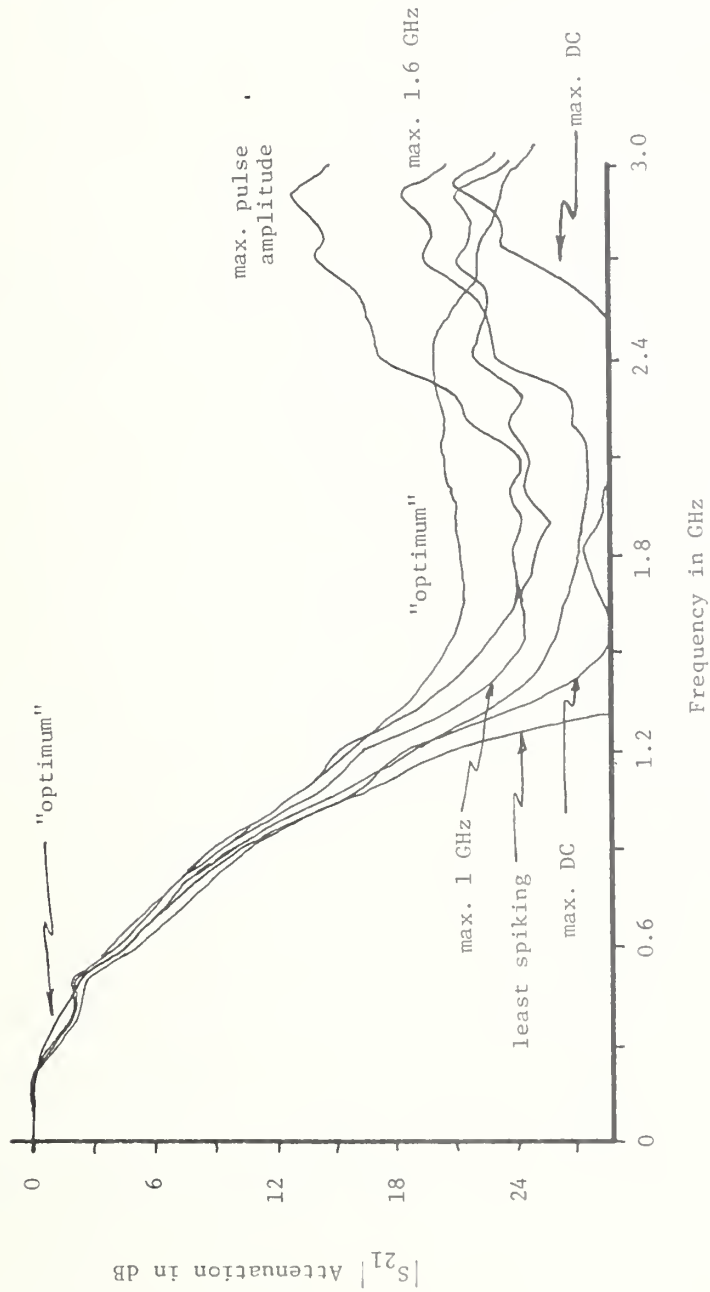


Figure 22. Frequency responses of the 580 m graded index fiber at 1.06 μm for various input launching conditions.

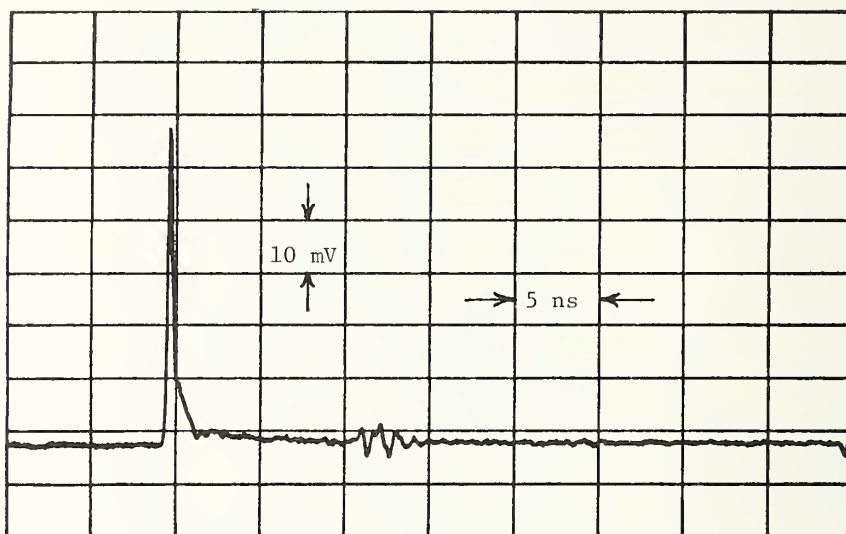


Figure 23. Test impulse from diode A.

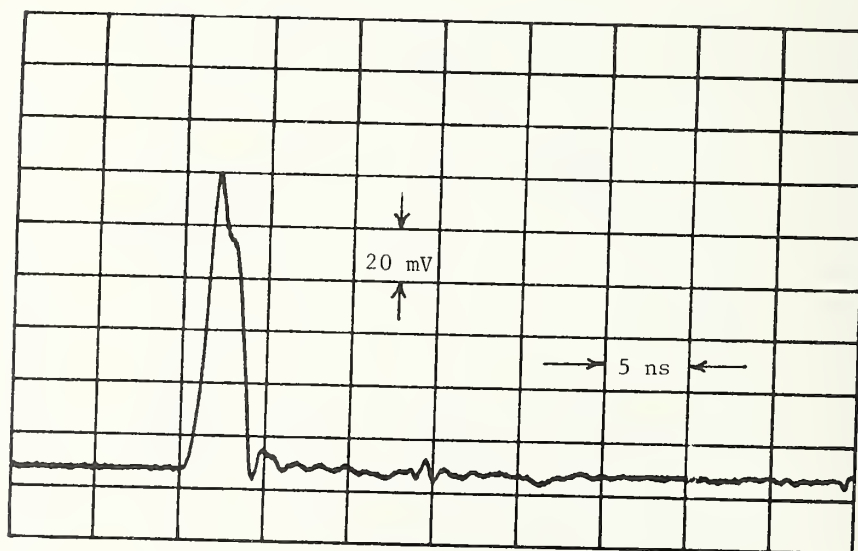


Figure 24. Impulse response of avalanche photodiode E.

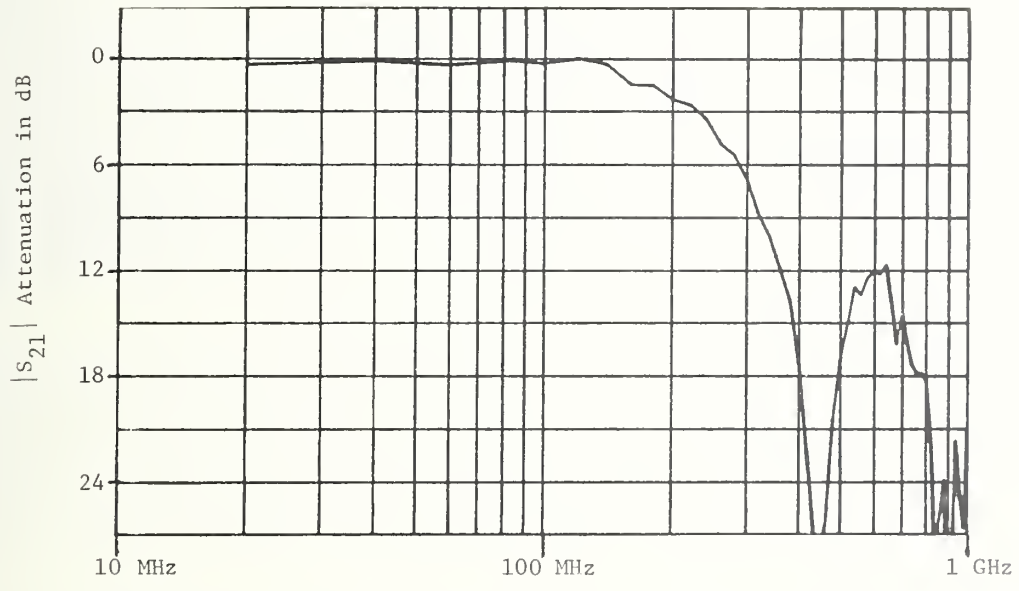


Figure 25. Frequency response of avalanche photodiode E.



FIG. 2. Photograph of GaAs laser diode pulse generator.

a slower pulse of 10 nsec transition time. It is necessary to limit the maximum pulse repetition rate to avoid exceeding the duty cycle limitations of the laser diode and the avalanche transistor. The maximum duty cycle is 0.1% for the laser diode and 0.05% for the transistor.

The actual circuit construction is shown in Fig. 2. It is constructed entirely over a rigid copper ground plane, such as a copper clad circuit board. This ground plane is bolted onto the optical bench. The $5\ \Omega$ microstrip transmission line *DL1* consists of a 1.27 cm wide strip of $76\ \mu$ thick FEP tape and a 1.27 cm wide strip of copper tape mounted directly on the ground plane. The FEP and copper tape assembly is held in place by a covering of 1.9 cm wide adhesive tape. The laser diode is mounted in an 8-32 nut that is soldered at a right angle to the ground plane. All of the other components are soldered in place using their own leads for support. All components are positioned very close

to the ground plane. All leads are cut to the shortest possible lengths to minimize parasitic lead inductances. These precautions are necessary to obtain a fast transition time with this very low impedance ($5\ \Omega$) circuit. The shields for the $50\ \Omega$ coaxial cables are also soldered directly to the ground plane. The cost of this generator, including the laser diode, is less than \$30.00.

When GaAs injection laser diodes are subjected to a fast-rising steplike injection current pulse, they have been observed to exhibit two phenomena in their optical output.⁸ The first is a delay in the optical output of the order of several nanoseconds after the injection current has reached the lasing threshold I_{th} . The second is Q-switching exhibited as a damped oscillation of the optical output with resonant frequency of the order of 1.5 GHz. Both of these phenomena may be observed when using this generator.

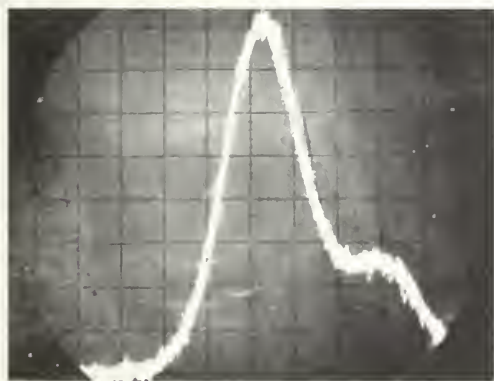


FIG. 3. Detected output from Ta-7606 GaAs laser diode. Single Q-switched impulse operation. Vertical scale is 5 mV/div. Horizontal scale is 50 psec/div.

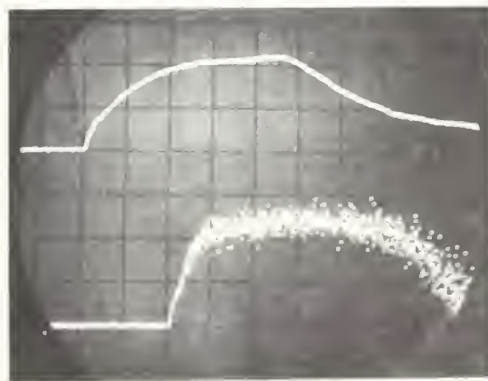


FIG. 4. Long pulse operation of GaAs laser diode. Top trace is diode injection current at 4.25 A/div. Bottom trace is detected output at 400 mV/div. Horizontal scale is 2 nsec/div.

For an application requiring a single narrow optical impulse, such as pulse dispersion studies in optical waveguides, the Q-switching may be used to advantage. If the duration of the injection current pulse is successively shortened, a point will be reached in which only the first pulse in the Q-switched train is excited. The actual duration of the optical impulse will vary depending upon the laser diode. Thus to obtain a very narrow impulse it may be necessary to make a selection of the best diode among a purchased lot.

With this generator and a TA-7606 laser diode the result shown in Fig. 3 was obtained. In this case the length of charge line, *DL1*, used was 20 cm. The maximum pulse repetition rate was 50 kHz. The photodiode used was an experimental diode.⁶ A 28 psec transition time sampling oscilloscope was used for the measurement. The observed impulse duration (50% level) is 110 psec. Some SG-2001's have been found to give similar results.

For relatively long optical pulses, it is necessary to simply increase the length of the charge line. The results

for a length of 1 m are shown in Fig. 4. The injection current waveform 10%-90% transition time is 4 nsec. The detected optical output shows the laser delay, Q switching, and multiple filament lasing. The maximum pulse repetition rate for this particular generator was 5 kHz.

This paper has presented an inexpensive GaAs laser diode pulse generator with application in optical waveguide studies. It is capable of producing optical impulses as narrow as 110 psec at a wavelength of 0.9μ and a pulse repetition rate of 50 kHz.

*Contribution of National Bureau of Standards.

¹W. A. Gambling, *Electron. Power* **18**, 446 (1972).

²E. A. Torrero, *Electron. Des.* **30** (1972).

³Remy Bouillie and James R. Andrews, *Electron. Lett.* **8**, No. 12, 309 (1972).

⁴James R. Andrews, *QST* **56**, No. 5, 16 (1972).

⁵M. J. Adams, S. Gründorfer, B. Thomas, Caroline F. L. Davies, and D. Mistry, *IEEE J. Quantum Electron.* **QE-9**, No. 2, 328 (1973).

⁶L'Echo des Recherches (Centre National D'Études des Télécommunications, Issy-les-Moulineaux, France, 1972), p. 55.

APPENDIX B

GaAs Laser Diode Pulse Generator (modified)

The GaAs laser diode pulse generator [9] described in Appendix A has been used at NBS for several years. However, due to variations in avalanche transistors and laser diodes the need was felt for some time to modify the previous circuit to allow for adjustment of the pulse duration of the pump current. This was necessary to insure excitation of a single optical pulse. With too long a current pulse, laser A will produce a train of relaxation oscillations at approximately a 3 GHz rate.

Figure B-1 is the circuit diagram of the modified, avalanche transistor pulser. It should be compared with figure 1 in Appendix A. The major changes are (1) that the 5 ohm delay line DL1 has been replaced with capacitors (C4-C7) and (2) that emitter resistor R5 has been deleted. The use of capacitors and the elimination of the emitter resistor allows a larger initial surge current into the laser diode CR1. Other workers have reported compact pulsers using ceramic-chip capacitors instead of transmission lines [3, 19]. The physical mounting configuration is similar to that used in Appendix A. All wiring leads are kept extremely short to minimize the circuit inductance. Likewise the array of four capacitors (C4-C7) is used instead of a single capacitor to minimize inductance. C7 is a variable capacitor to permit minor adjustment of the pump current duration. Variation of the B+ voltage permits minor adjustment of the pump current's magnitude.

As noted in Appendix A, it is necessary to select the avalanche transistor Q1 and the laser diode CR1 to optimize performance. In particular, the higher the breakdown voltage, BV_{CER} , the greater the pump current will be. If a particular laser when pulsed produces more than one relaxation oscillation, then the value of C7 should be reduced. If there is not enough adjustment range then the other capacitors, C4-C6, can be increased or decreased as needed.

A 50 ohm coaxial cable is used as a probe to monitor the voltage across the laser diode CR1. Figure B-2 shows a typical voltage waveform at this test point.

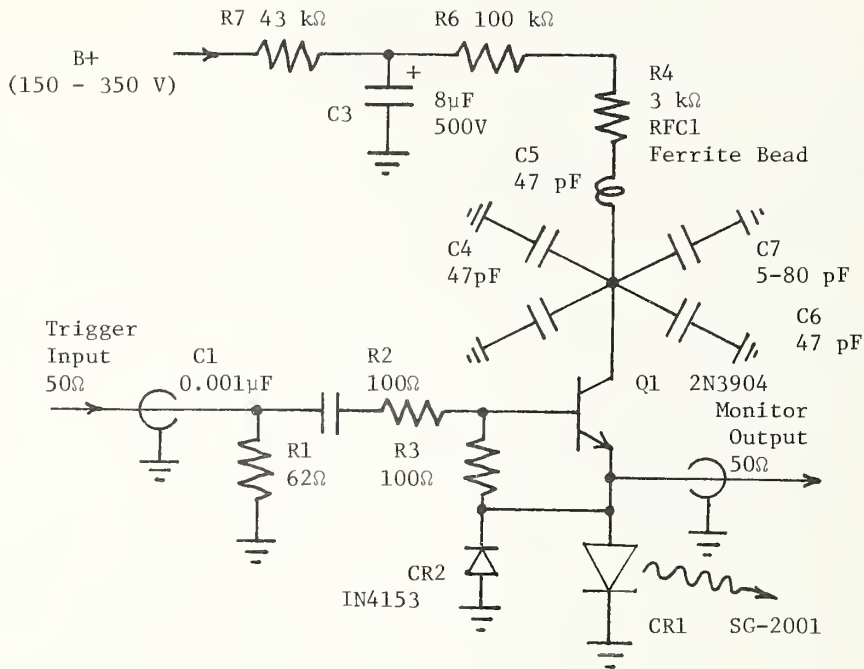


Figure B-1. Modified avalanche transistor pulser for GaAs laser diode.

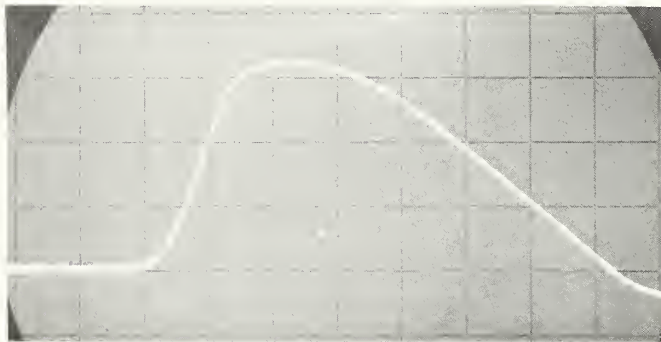


Figure B-2. Typical operation. Voltage waveform across the laser diode. Vert. 10V/cm, Horiz. 500 ps/cm.

REFERENCES

- [1] Andrews, James R., Measurement of laser pulse dispersion in glass fiber optical waveguides, NBS Memorandum for the Record, NBS, Boulder, Colo., (July 1972).
- [2] Nelson, B. P. and Stern, J. R., Pulse propagation measurements on slightly overmoded glass fibers, 1st European Conference on Optical Fibre Communications, London, Sept. 16-18, 1975, 13-15.
- [3] Dannwolf, J. W., et al., Optical-fiber impulse-response measurement system, IEEE Trans. on Inst. & Meas., IM-25, No. 4, Dec. 1976, 401-406.
- [4] Gans, W. L., et. al., Applications of an automated pulse measurement system to telecommunication measurements, Conference sur la Mesure dans les Télécommunications, URSI, Lannion, France, (October 1977), 165-170.
- [5] Andrews, J. R., Automatic network measurements in the time domain, Proc. IEEE, 66, No. 4, (April 1978), 414-423.
- [6] Ramirez, R. W., Evaluating fibers digitally, Laser Focus, (April 1979), 46-52.
- [7] Mil-Std-1678, Military Standard - Fiber optics test methods and Instrumentation, draft version, 17 Dec. 1976, Method 6050, Pulse Spreading, pp. 6050-1 to 7.
- [8] Andrews, J. R., Light impulses from GaAs injection diode lasers, talk presented at Fibre Optical Communication Meeting, London, March 28, 1972.
- [9] Andrews, James R., Inexpensive laser diode pulse generator for optical waveguide studies, Rev. Sci. Instrum. 45, No. 1, (Jan. 1974), 22-24.
- [10] Greenhow, R. C., and Schmidt, A. J., Picosecond Light Pulses, in Advances in Quantum Electronics, 2, edited by D. W. Goodwin, Academic Press, New York, London, 1974.
- [11] Young, M., Optics and Lasers, An Engineering Physics Approach, Springer, New York, Berlin, Heidelberg, 1977, Chapters 2, 5.
- [12] Détection des impulsions lumineuses issues d'un laser YAG par tête de détection au germanium, L'Echo des Recherches, CNET, Issy-les-Moulineaux, France, (July 1972), 55.
- [13] Gans, W. L., Present capabilities of the NBS automatic pulse measurement system, IEEE Trans. Inst. & Meas., IM-25, 4, (Dec. 1976), 384-388.
- [14] Guillaume, M. E. and Nahman, N. S., Deconvolution of Time Domain Waveforms, NBSIR 79- , National Bureau of Standards, Boulder, Colorado, 1979. In progress.
- [15] Kao, C., Estimating the dispersion effects in a practical multimode waveguide cable for fiber systems, 1st European Conference on Optical Fibre Communication, IEE, London, (Sept. 1975), 8-10.
- [16] Gambling, W. A. and D. N. Payne, Some experimental aspects of propagation in optical fibres, 1st European Conference on Optical Fibre Communications, IEE, London, (Sept. 1975), 197-200.
- [17] Okamoto, K., Comparison of calculated and measured impulse responses of optical fibers, Applied Optics, 18, No. 13, (July 1, 1979), 2199-2206.
- [18] Olshansky, R. and Keck, D. B., Pulse broadening in graded-index optical fibers, Appl. Opt., 15, (1976), 483-491.
- [19] Vanderwall, J. et. al., Subnanosecond rise time pulses from injection lasers, IEEE, J. Quantum Electronics, July 1974, pp. 570-572.

U.S. DEPT. OF COMM. BIBLIOGRAPHIC DATA SHEET	1. PUBLICATION OR REPORT NO. NBSIR 79-1620	2. Gov't. Accession No.	3. Recipient's Accession No.
4. TITLE AND SUBTITLE TIME DOMAIN PULSE MEASUREMENTS AND COMPUTED FREQUENCY RESPONSES OF OPTICAL COMMUNICATIONS COMPONENTS		5. Publication Date September 1979	
7. AUTHOR(S) James R. Andrews and Matt Young		6. Performing Organization Code	
9. PERFORMING ORGANIZATION NAME AND ADDRESS NATIONAL BUREAU OF STANDARDS DEPARTMENT OF COMMERCE WASHINGTON, DC 20234		8. Performing Organ. Report No.	
12. SPONSORING ORGANIZATION NAME AND COMPLETE ADDRESS (Street, City, State, ZIP)		10. Project/Task/Work Unit No.	
15. SUPPLEMENTARY NOTES <input type="checkbox"/> Document describes a computer program; SF-185, FIPS Software Summary, is attached.		11. Contract/Grant No.	
16. ABSTRACT (A 200-word or less factual summary of most significant information. If document includes a significant bibliography or The purpose of this report is to demonstrate the application of the NBS Automatic Pulse Measurement System (APMS) to measuring the pulse responses of optical communications components and to computing their impulse and frequency responses. For example we describe measurements of the properties of two glass fibers and an avalanche photodiode using both a pulsed GaAs laser diode ($\lambda = 0.9 \mu\text{m}$) and a mode locked, Nd:YAG laser ($\lambda = 1.06 \mu\text{m}$). All measurements were performed in the time domain; frequency domain data were obtained from the time domain data by using the Fast Fourier Transform (FFT). The impulse response was obtained by deconvolution.		13. Type of Report & Period Covered	
17. KEY WORDS (six to twelve entries; alphabetical order; capitalize only the first letter of the first key word unless a proper name; separated by semicolons) Avalanche photodiode; FFT; fiber optics; Frequency response; impulse response; laser; photodiode		14. Sponsoring Agency Code	
18. AVAILABILITY <input checked="" type="checkbox"/> Unlimited <input type="checkbox"/> For Official Distribution. Do Not Release to NTIS <input type="checkbox"/> Order From Sup. of Doc., U.S. Government Printing Office, Washington, DC 20402, SD Stock No. SN003-003- <input checked="" type="checkbox"/> Order From National Technical Information Service (NTIS), Springfield, VA, 22161	19. SECURITY CLASS (THIS REPORT) Unclassified UNCLASSIFIED 20. SECURITY CLASS (THIS PAGE) UNCLASSIFIED	21. NO. OF PRINTED PAGES 22. Price	

NBSIR 79-1620